A THESIS FOR THE DEGREE OF MASTER OF SCIENCE

Characterization of emulsion-filled chitosan-pectin hydrogel prepared by cold-set gelation

Cold-set 겔화에 의해 제조된 에멀젼 함입 키토산/펙틴 하이드로겔의 특성연구

August, 2021

Department of Agricultural Biotechnology

Seoul National University

Huisu Kim

석사학위논문

Characterization of emulsion-filled chitosan-pectin hydrogel prepared by cold-set gelation

지도교수 장 판 식

이 논문을 석사학위 논문으로 제출함

2021년 8월

서울대학교 대학원

농 생 명 공 학 부

김 희 수

김희수의 석사 학위논문을 인준함

2021년 8월

위원장 최 영 진

부위원장 장 판 식

위원 유 상 열

Abstract

Oil-in-water (O/W) emulsions are widely utilized as a carrier for a lipophilic bioactive compound. However, destabilization of emulsion occurs during digestion, affecting on bioaccessibility of the lipophilic compound. Recently, delivery systems have been developed to improve the stability of emulsion within gastrointestinal (GI) tract and enhance the bioaccessibility of bioactive compounds. In this study, emulsion-filled hydrogel (EFH) was prepared through cold-set gelation under acidic conditions without any chemical agents. Chitosan and pectin were used as a hydrogel matrix and sodium caseinate as an emulsifier. The oscillation frequency sweep test showed that the elasticity (G') increased as pectin concentration increased (0.75-1.50%, w/v). Moreover, all EFH exhibited weak gel properties. Scanning electron microscope was used to observe the changes in the structure of EFH with different pectin concentrations. The microstructure of EFH showed that pore size decreased as the pectin concentration increased, indicating that the hydrogel networks of EFH became more compact as pectin concentration increased. FT-IR analysis was used to verify the interaction between chitosan and pectin in EFH. The hydrogen bond and electrostatic interaction between chitosan and pectin are assigned to 3,326 cm^{-1} and 1,500-1,600 cm^{-1}, respectively. There was no significant difference

depending on the presence or absence of the emulsion in the range from 1,500 to 1,800 cm^{-1}, suggesting that the addition of emulsion did not affect the interaction between the polymers, which constitutes the hydrogel matrix. Release profile of emulsion indicated that the hydrogel matrix prevented the release of emulsion at pH 2.0. On the other hand, the emulsion was released at pH 7.4. Moreover, release rate and release amount of emulsion were influenced by the pectin concentration. The release of emulsion reduced as pectin concentration increased. During *in vitro* digestion, the free fatty acid release in EFH was 58.67, 55.88, 48.87, and 43.76% at pectin concentrations of 0.75, 1.00, 1.25, and 1.50%, respectively. The amount of free fatty acids was decreased as the pectin concentration increased. Compared with emulsion, the free fatty acid release in EFH with 0.75% pectin was significantly higher than that of emulsion ($p < 0.05$). Confocal laser scanning microscopy images showed that the hydrogel matrix protected the emulsion from destabilization within the oral and gastric stages. The bioaccessibility of curcumin, a model lipophilic compound, decreased as the pectin concentration increased, and the bioaccessibility in EFH with 0.75% pectin (23.95 ± 0.8%) was 1.38 fold higher than that in emulsion (17.25 ± 2.1%). Therefore, this study demonstrated that EFH improves emulsion stability in GI tract and enhances the bioaccessibility of lipophilic compound. Therefore,

EFH is a potential carrier system for lipophilic bioactive compounds in the food industry.

Keywords: chitosan, pectin, emulsion-filled hydrogel, delivery system, sodium caseinate emulsion, bioaccessibility

Student number: 2019-21740

Contents

List of Tables

List of Figures

Fig. 5. SEM images of EFH with different pectin concentrations (a) 0.75%, (b) 1.00%, (c) 1.25%, and (d) 1.50% (w/v).

Fig. 6. FT-IR spectra of (a) chitosan, (b) pectin, (c) EFH, and (d) hydrogel without emulsion.

Fig. 7. Release properties of emulsion from hydrogel matrix. (a) Visual appearance of EFH with 0.75% (w/v) pectin after exposed to medium at pH 2.0 and 7.4 for 2 h and (b) the release profiles of emulsion depending on pectin concentrations (0.75-1.50%, w/v) at pH 2.0 and 7.4.

Fig. 8. The effect of salt concentration (0-200 mM) on emulsion release from hydrogel matrix with 0.75% pectin in 100 mM sodium phosphate buffer at pH 7.4 for 2 h.

Fig. 9. Release profiles of FFA from EFH and sodium caseinate emulsion measured using a pH-stat during small intestinal stage.

Fig. 10. CLSM images of EFH with different pectin concentrations (0.75-1.50%, w/v) and sodium caseinate emulsion after digestion at oral and gastric stage. (a) Sodium caseinate emulsion, (b) EFH with 0.75% pectin, (c) EFH with 1.00% pectin, (d) EFH with 1.25% pectin, and (e) EFH with 1.50% pectin. The scale bar is 5.0 μm.

Fig. 11. Bioaccessibility of curcumin in sodium caseinate emulsion and EFH with different pectin concentrations (0.75-1.50%, w/v).

1. Introduction

Oil-in-water (O/W) emulsions are widely used for encapsulating lipophilic bioactive compounds such as carotenoids, phytosterols, and curcuminoids (Araiza-Calahorra, Akhtar, & Sarkar, 2018; McClements, Decker, & Weiss, 2007; Raikos & Ranawana, 2017). Sodium caseinate, well-known as a food-grade dairy protein, has been utilized in food industry as an emulsifier. Compared with other protein emulsifiers, it has heat-resistant properties because the relatively flexible casein molecules are less susceptible to heat-induced conformational changes (Ma & Chatterton, 2021; Perugini, Cinelli, Cofelice, Ceglie, Lopez, & Cuomo, 2018; Salminen, Bischoff, & Weiss, 2019). Nevertheless, destabilization of sodium caseinate emulsion can be occurred during digestion, which is caused by protease presented in gastric fluid. The interfacial protein layer of emulsion is broken down and converted into peptides which are not strong enough to offer emulsion stability during the gastric digestion, changing the size and microstructure of the emulsion (J. Li, Ye, Lee, & Singh, 2012). The changes in droplet size reduce the access of lipase to the oil-water interface, resulting in low bioaccessibility of lipophilic bioactive compounds (Yi, Li, Zhong, & Yokoyama, 2014).

Emulsion-filled hydrogel (EFH) consisting of one or more hydrophilic polymers is a three-dimensional network, in which emulsions are trapped inside the hydrogel matrix (Araiza-Calahorra et al., 2018; Farjami & Madadlou, 2019; Lu, Zhang, Yuan, Gao, & Mao, 2021). Lipid digestion and release of encapsulated compounds in emulsion can be controlled by hydrogel matrix in the gastrointestinal tract (McClements & Li, 2010). Moreover, the hydrogel matrix prevent the emulsion destabilization during the digestion, resulting in improving bioaccessibility of the compounds (Lu et al., 2021; Matalanis & McClements, 2012; Mun, Kim, Shin, & McClements, 2015). Ionically cross-linked hydrogel has been widely used in food industries as drug delivery systems (Jain, Winuprasith, & Suphantharika, 2020; Y. Li, Hu, Du, Xiao, & McClements, 2011; Silva, Bourbon, Pastrana, & Sato, 2020). However, the cross-linked hydrogels have low stability in the presence of monovalent ions and calcium-sequestering agents (Lee & Mooney, 2012; Sarker et al., 2014). The other cross-linkers such as glutaraldehyde and carbodiimide, used for preparing hydrogel, have cytotoxic properties to humans (Ulubayram, Aksu, Gurhan, Serbetci, & Hasirci, 2002).

Chitosan and pectin have been commonly used for hydrogel preparation in

food and biomedical fields, due to their biocompatible, biodegradable, and non-toxic characteristics. Chitosan/pectin hydrogel-based carrier systems, allowing to control release of bioactive compounds, has been proposed in several studies (Maciel, Yoshida, & Franco, 2015; Neufeld & Bianco-Peled, 2017). Moreover, chitosan/pectin hydrogels can be prepared without any chemical agents for cross-linking between the polymers, which has little safety concerns. This hydrogel can be prepared via physical interaction (*i.e.* hydrogen bond) between polymers by lowering the pH below pK_a of chitosan and pectin (Marianne H. Nordby, 2003; Ventura & Bianco-Peled, 2015).

The objective of this study is to prepare EFH using chitosan and pectin to enhance emulsion stability in gastrointestinal tract, thereby improving bioaccessibility of lipophilic bioactive compounds. EFH containing sodium caseinate emulsion was fabricated based on cold-set gelation method without any chemical agents. To evaluate the physicochemical properties of EFH, its rheological properties and microstructure were determined. The gastrointestinal behaviors of EFH, including free fatty acid release and bioaccessibility of curcumin as a model lipophilic bioactive compound, were investigated using *in vitro* digestion model.

2. Material and methods

2.1. Material

Chitosan from shrimp shells with low viscosity, pectin from citrus peel, casein sodium salt from bovine milk, pepsin from porcine gastric mucosa powder (≥ 250 units/mg solid), bile extract porcine, mucin from porcine stomach (Type II), pancreatin from porcine pancreas (8 × USP specifications), and curcumin from *Curcuma longa* were purchased from Sigma-Aldrich (St. Louis, MO, USA). Soybean oil was purchased from Daejung Chemicals (Siheung, Republic of Korea). All other chemicals were of analytical grade.

2.2. Preparation of emulsion-filled hydrogel

2.2.1. Emulsion

Sodium caseinate solution was prepared by dissolving 1.0% (w/v) of sodium caseinate in deionized water. Then, soybean oil of 1.0 g was added into 9.0 g of the sodium caseinate solution. Coarse emulsion was prepared by using a homogenizer (ULTRA-TURRAX IKA T18 Basic with S25N-10 G, IKA Works Inc., Wilmington, NC, USA) at 11,000 rpm for 1 min. After the homogenization, the coarse emulsion was sonicated to make fine emulsions

for 5 min (5 s on and 5 s off) at 30% power by ultrasonicator (Sonomasher, S&T Science, Seoul, Republic of Korea). Curcumin loaded emulsion was prepared by dissolving curcumin in oil at 0.1% (w/w) with the same manners.

2.2.2. Emulsion-filled hydrogel

EFH was prepared by cold-set gelation at low pH conditions. Chitosan was dissolved at concentration of 2.0% (w/v) in 0.1 M HCl by magnetic stirring at 500 rpm for 12 h, and then mixed with emulsion at 1:1 (v/v) ratio. Pectin solutions were prepared by dissolving 1.5, 2.0, 2.5, and 3.0% (w/v) of pectin in 0.05 M HCl by magnetic stirring at 500 rpm for 6 h at 60℃, respectively. After that, the mixture of chitosan and emulsion was heated at 60℃ for 1 h, and mixed with pectin solution at 1:1 (v/v) ratio using a magnetic stirrer at 500 rpm for 1 h at 60℃. After that, the mixture were poured into a silicone square mould (3.0 cm × 3.0 cm) and stored at 4℃ until use.

2.3. Rheological properties of emulsion-filled hydrogel

2.3.1. Oscillation frequency sweep test

The rheological properties of EFH were carried out by using a dynamic shear rheometer (Rheostress RS 1; HAAKE Instruments, Karlsruhe, Germany) with a plate-plate geometry (PP20 Ti, diameter 20.0 mm; gap size

4.0 mm). Prior to analysis, samples were loaded between parallel plates and equilibrated at 20°C for 10 min. The storage modulus (G') and loss modulus (G'') were obtained over a frequency range of 0.01-1.00 Hz with stress amplitude of 1.00 Pa (in linear viscoelastic region). Paraffin oil was used to prevent water evaporation during the measurement. The oscillation time sweep test was performed with 1.00 Hz and 1.00 Pa for 3 h. Other conditions were same to describe above.

2.3.2. Texture profile analysis (TPA)

EFH was analyzed by CT3 Texture analyzer (Brookfiled, USA) equipped with a measuring cylinder probe (diameter of 50.0 mm). Samples were cut into small blocks (1.5 cm × 1.5 cm) and compressed twice with 50% deformation at a constant probe speed of 1.0 mm/s. Data of hardness, adhesiveness, fracturability, and springiness were collected by the software provided with the manufacture.

2.4. Scanning electron microscopy (SEM)

To evaluate the effect of pectin concentrations on the microstructure of EFH, EFH was lyophilized in freeze dryer (FD8512, Iishin Co., Dongducheon, Republic of Korea) for 2 days to obtain dried samples. The samples were placed on a copper stub and sputtered with platinum. All images were obtained by field-emission scanning electron microscope (SIGMA, Carl Zeiss, UK) at an accelerating voltage of 5.0 kV.

2.5. Fourier-transform infrared spectroscope (FT-IR)

To analyze the chemical interaction of polymers in hydrogel, FT-IR analysis was carried out by using FT-IR spectrophotometer (Nicolet 6700, Thermo Scientific, USA) operating in the ATR mode equipped with window ZnSe/diamond. EFH and hydrogel without emulsion were lyophilized by the procedure described in section 2.4. Data collection was performed in the range of 650-4,000 cm^{-1} with a 4 cm^{-1} spectral resolution and number of 64 scans.

2.6. Release profile of emulsion from hydrogel matrix

The release profile of emulsion was carried out according to the previous method (Lim, Ho, Surjit Singh, Ooi, Tey, & Chan, 2020; Surjit Singh, Lim, Tey, & Chan, 2021) with slight modification. Neutral medium (100 mM PBS; pH 7.4) and the acidic medium (100 mM PBS; pH 2.0) were used to evaluate the release properties depending on pH. EFH sample was suspended in 100.0 mL of the acidic medium for 2 h. After that, samples were removed from the acidic medium and transferred into 100.0 mL of the neutral medium. The experiments were carried out with agitation at 100 rpm and 37℃ in shaking incubator. At pre-determined time, 2.0 mL of the medium was collected and replaced with equal volume of fresh medium to maintain the sink condition. The turbidity of aliquots was measured by UV-Vis spectrophotometer at 600 nm (Optizen POP-BIO, Mecasys Co., Ltd., Daejeon, Republic of Korea). The release percentage of emulsion was calculated from turbidity of emulsion in calibration curve (R^2 = 0.9985).

2.7. Confocal laser scanning microscopy (CLSM)

EFH in the different digestion stages was observed by confocal laser scanning microscopy (SPX 8, Leica, Mannheim, Germany) with confocal scan objectives (HC PL APO 63x/1.4 Oil CS2). The oil phase was dyed by

dissolving Nile red 0.01% (w/v) in soybean oil. Initial samples before digestion and the samples from the digestion stages were placed on slide glass and coated with cover slip before observation. The white light laser set at 550 nm to excite the Nile red and emission wavelength was 580 nm.

2.8. *In vitro* digestion model

The *in vitro* digestion model was prepared according to the methods described in previous studies with slight modification (Lei, Zhang, He, Wu, Li, & Li, 2017; Mun et al., 2015). Emulsion and EFH containing curcumin were passed through simulated gastrointestinal tract which consists of an oral phase, a gastric phase, and a small intestine phase in a sequential manner.

Oral phase: simulated saliva fluid consisted of mucin and various salts was prepared according to previous study (Sarkar, Goh, & Singh, 2009). EFH was cut into small blocks to simulate oral break down (5.0 mm × 5.0 mm) and emulsion was diluted 4-fold with distilled water before digestion, and then 7.5 g samples containing 187.5 mg oil were put into saliva fluid. The volume ratio of saliva and sample was 1:1 and the total volume was 15.0 mL. The pH of the mixture was adjusted to 6.8 using 1 M NaOH and then incubated in shaking incubator (37℃) for 5 min with 100 rpm (VS-8480SF, Vision Co. Republic of Korea).

Gastric phase: simulated gastric fluid (SGF) was prepared by dissolving 2.0 g of NaCl and 7.0 mL of HCl in 1.0 L distilled water. SGF containing 3.2 g/L pepsin was pre-incubated for 10 min and mixed with samples from the oral phase at 1:1 (v/v) ratio. Then pH was adjusted to 2.5 using 1 M NaOH and incubated with shaking (100 rpm) at 37℃ for 2 h to mimic the stomach conditions.

Small intestinal phase: The pH of sample (30.0 mL) from stomach phase was adjusted to 7.0 immediately using 1 M NaOH. After that, 1.5 mL of salt solution containing 10 mM calcium chloride and 150 mM sodium chloride was added into mixture. Then, 3.5 mL of bile extract solution (53.5 mg/mL in 10 mM sodium phosphate buffer) was added to the reaction vessel. Pancreatin solution was prepared by dissolving in 75.0 mg/mL in 10 mM sodium phosphate buffer (pH 7.0). The pancreatin solution of 2.5 mL (pre-heated at 37℃ for 20 min) was added and the pH of reaction vessel was maintained at pH 7.0 using an automatic titration unit (842 Titrando; Metrohm AG, Herisau, Switzerland) with 0.05 M NaOH. The free fatty acids (FFA) release from the digestion was recorded for 2 h and quantified by following equation.

$$\text{FFA release (\%)} = (V_{NaOH} \times m_{NaOH} \times M_{Lipid} / W_{Lipid} \times 2) \times 100$$

Where, V_{NaOH} is the volume of NaOH used to neutralize the FFA produced, m_{NaOH} is the molarity of NaOH (0.05 M), M_{Lipid} is the molecular weight of soybean oil (920.0 g/mol), and W_{Lipid} is the weight of the lipid initially added into reaction vessel (187.5 mg). V_{NaOH} of blank prepared without oil was subtracted from that of samples to exclude any pH change due to other factors.

2.9 Bioaccessibility determination

After small intestinal digestion, the bioaccessibility of curcumin, as a model lipophilic bioactive compound, was determined by using the method described previously with slight modification (Pan et al., 2019). Briefly, the digesta was centrifuged at 110,000 ×g for 40 min at 20℃ (Himac CP100β with P40ST rotor, Hitachi, Japan), followed by micelle phase was collected by using 5.0 mL syringe. Micelle phase (2.0 mL) was mixed with chloroform at 1:2 (v/v) ratio, and then centrifuged at 3,000 ×g (Labogene 1236R, Gyrozen Co., Daejeon, Republic of Korea) for 10 min. The bottom layer of chloroform was aliquoted. The absorbance of chloroform phase was measured using spectrophotometer (Optizen POP-BIO, Mecasys Co., Ltd., Daejeon, Republic of Korea) at 420 nm. The content of curcumin was determined by standard curve of curcumin in chloroform (R^2 = 0.9998). The

bioaccessibility of curcumin was calculated by the following equation.

$$\text{Bioaccessibility (\%)} = (C_{micelle} / C_{initial}) \times 100$$

Where, $C_{micelle}$ and $C_{initial}$ represent a concentration of curcumin in micelle phases and initial concentration of curcumin before digestion, respectively.

2.10. Statistical analysis

All data were represented as means and standard deviations of triplicate experiments, and performed by analysis of variance (ANOVA) using SPSS software version 19 (SPSS, Inc., Chicago, IL, USA). The significance of differences was determined by using Duncan's multiple range test ($p < 0.05$).

3. Results and discussions

3.1. Fabrication of chitosan-pectin emulsion filled hydrogel

EFH was prepared by cold-set gelation using chitosan and pectin under the acidic condition (pH ≈ 1.7). While pectin concentration was fixed at 0.75% (w/v), EFH with different chitosan concentrations (0-0.75%, w/v) was prepared (Fig. 1a). It was found that only the hydrogel with 0.50% chitosan was in a solid state. On the other hand, at the chitosan concentrations of 0, 0.25, and 0.75%, the hydrogel was in a liquid state. At 0.75% chitosan, it was expected that chitosan molecules interfere the gel formation by electrostatic repulsion between chitosan molecules. Chitosan has a positive charge in the acidic condition (pH ≈ 1.7) due to its pK_a ranging from 6.2 to 7.1 (Kumar, 2000; Ventura et al., 2015). Thus, the concentration of chitosan was fixed at 0.50%.

The visual appearance of EFH with different pectin concentrations (0.50-1.50%, w/v) was observed (Fig. 1b). EFH with solid-like properties was formed at pectin concentrations from 0.75 to 1.50%. At 0.50% pectin, hydrogel was viscous solution, probably due to insufficient amount of pectin to form a continuous network with chitosan (Ventura et al., 2015).

Meanwhile, at a concentration higher than 1.50%, hydrogel was not formed since pectin was not completely dissolved (data not shown). As a result, for the preparation of EFH, concentrations of chitosan and pectin were set 0.50% and 0.75-1.50%, respectively.

The morphology of emulsion in the hydrogel matrix was observed by CLSM (Fig. 2). It was identified that the lipid droplets were uniformly distributed in EFH, regardless of pectin concentrations. These results suggested that the emulsion was embedded in the hydrogel matrix in intact states, indicating that there was no interaction between sodium caseinate emulsion and the hydrogel matrix. Since the isoelectric point of sodium caseinate is pH 4.7, the sodium caseinate emulsion is positively charged at below pH 4.0 (Ilyasoglu & El, 2014). Thus, the positively charged sodium caseinate and chitosan repulse each other, resulting in no phase separation or precipitation during the preparation. Moreover, the carboxyl groups of pectin are neutralized due to their pK_a value of 3.5, which does not cause electrostatic interaction with sodium caseinate (Clitor J. F. Souza & Garcia-Rojas, 2015).

(a)

Chitosan concentration (0-0.75%, w/v)

(b)

Pectin concentration (0.50-1.50%, w/v)

Fig. 1. Effects of pectin and chitosan concentrations on the formation of EFH. (a) Visual appearance of EFH with different chitosan concentrations at 0.75% pectin and (b) visual appearance of EFH with different pectin concentrations at 0.5% chitosan.

(a)

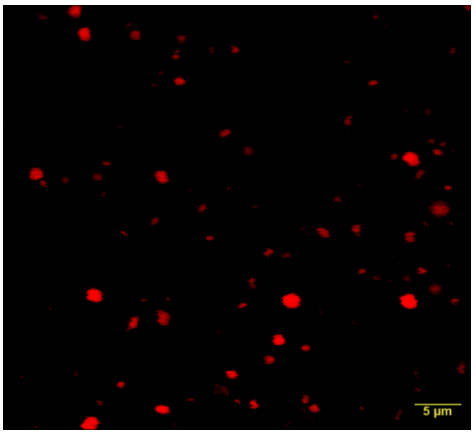

(b)

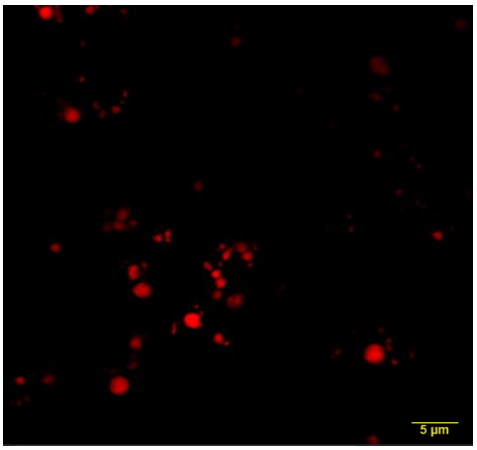

(c)

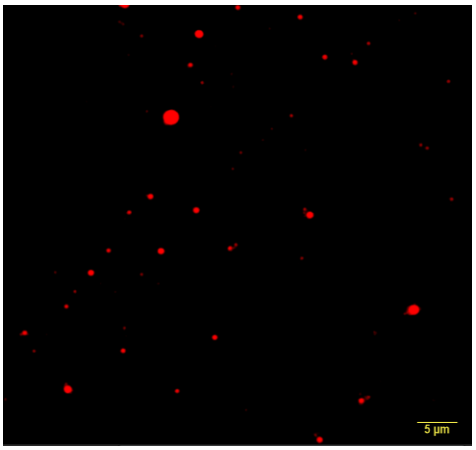

(d) (e)

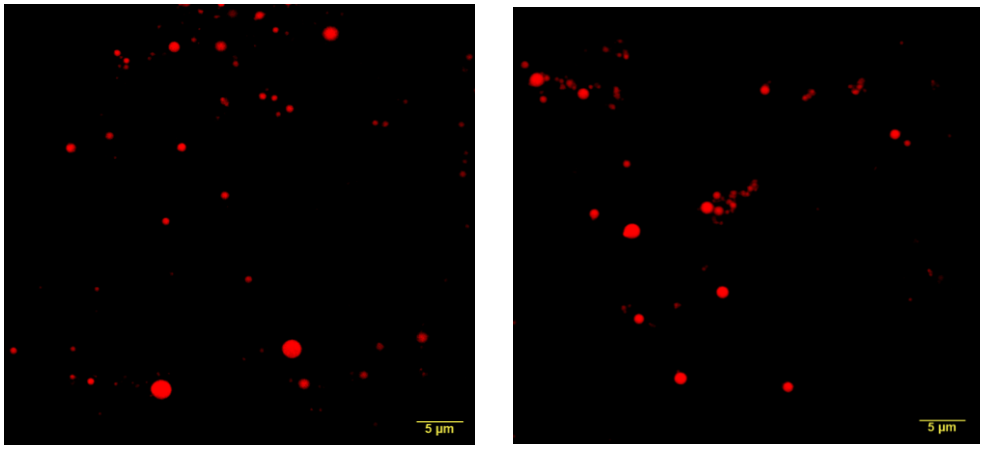

Fig. 2. CLSM images of sodium caseinate emulsion and EFH with different pectin concentrations (0.75-1.50%, w/v). (A) Sodium caseinate emulsion, (B) EFH with 0.75% pectin, (C) EFH with 1.00% pectin, (D) EFH with 1.25% pectin, and (E) EFH with 1.50% pectin.

3.2. Rheological properties of emulsion-filled hydrogel

The rheological properties of EFH were evaluated by oscillation measurements. The frequency sweep test was performed to observe the changes in viscoelastic behavior. As shown in Fig. 3a and 3b, all the samples showed that storage modulus (G') was higher than loss modulus (G") and frequency independent behavior (*i.e.* a plateau line over the frequency) in the frequency range (0.01-1.00 Hz). In addition, the storage modulus increased as the pectin concentration increased, which indicated that the increase in pectin concentration led to the formation of a more compact hydrogel. It is regarded that hydrogel has solid-like properties, when the values of loss angle (tan δ) of hydrogel is less than 1.00 (Hesarinejad, Koocheki, & Razavi, 2014). In all frequency ranging from 0.01 to 1.00 Hz, the tan δ was measured to be around 0.25, suggesting that EFH exhibits predominantly elastic behavior regardless of pectin concentrations (Fig. 3c). However, above 1.00 Hz, storage modulus and loss modulus became frequency dependent (data not shown), showing that EFH has weak gel properties (Tang, Du, Hu, Shi, & Kennedy, 2007).

In order to verify that EFH had solid-like properties, the time sweep test was performed (Fig. 4). All EFH exhibited a time-independent storage

modulus, and the storage modulus was higher than loss modulus over the entire shearing time. The tan δ of EFH were measured below 0.3, which indicates that the elastic response of EFH is higher than viscous response.

The textural parameters of EFH were analyzed by TPA (Table 1). As pectin concentration increased, significant increase in springiness were observed ($p < 0.05$), which was consistent with the rheological properties, showing the increase in elasticity with increasing pectin concentration. However, the hydrogel with different pectin concentrations showed no significant differences ($p < 0.05$) on fracturability, resilence, and hardness, indicating that EFH has poor mechanical properties due to reversible physical interactions (Parhi, 2017).

(a)

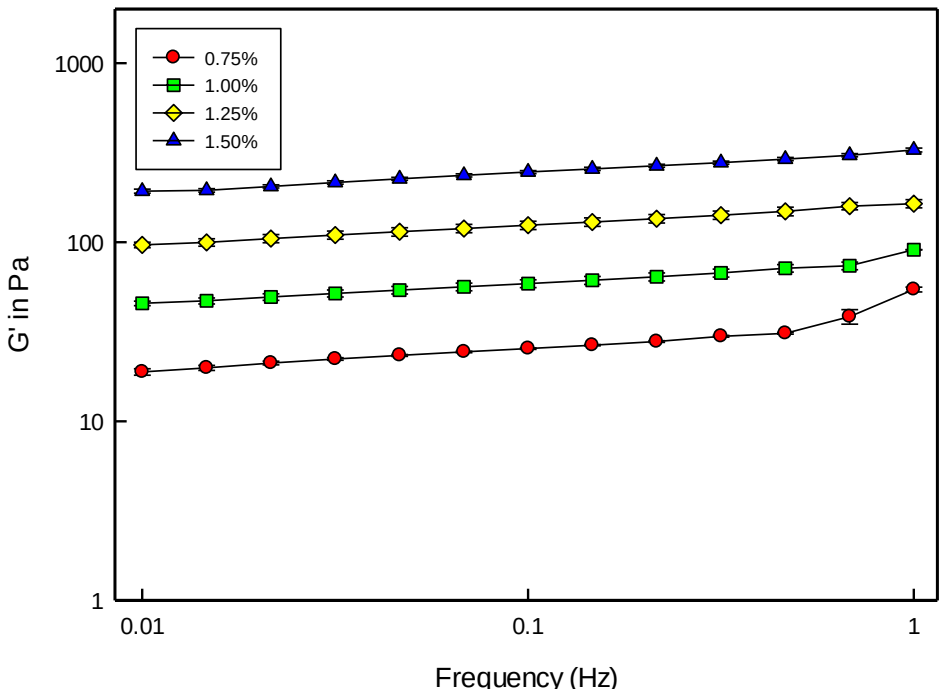
0.75%
1.00%
1.25%
1.50%
1000
100
10
1
G' in Pa
0.01
0.1
1
Frequency (Hz)

(b)

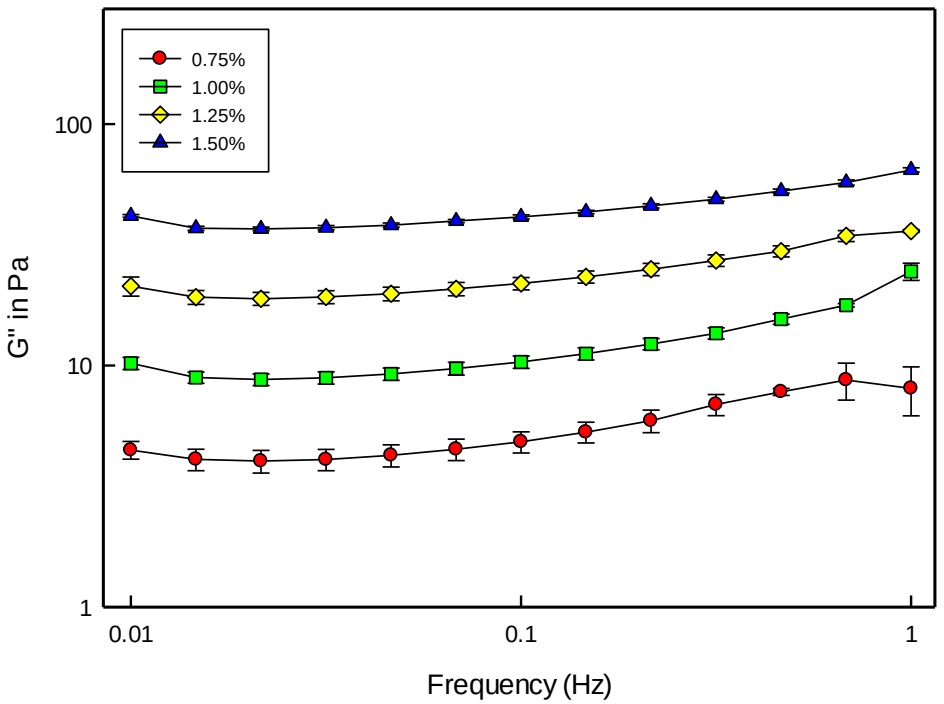
0.75%
1.00%
1.25%
1.50%
100
10
1
G'' in Pa
0.01
0.1
1
Frequency (Hz)

(c)

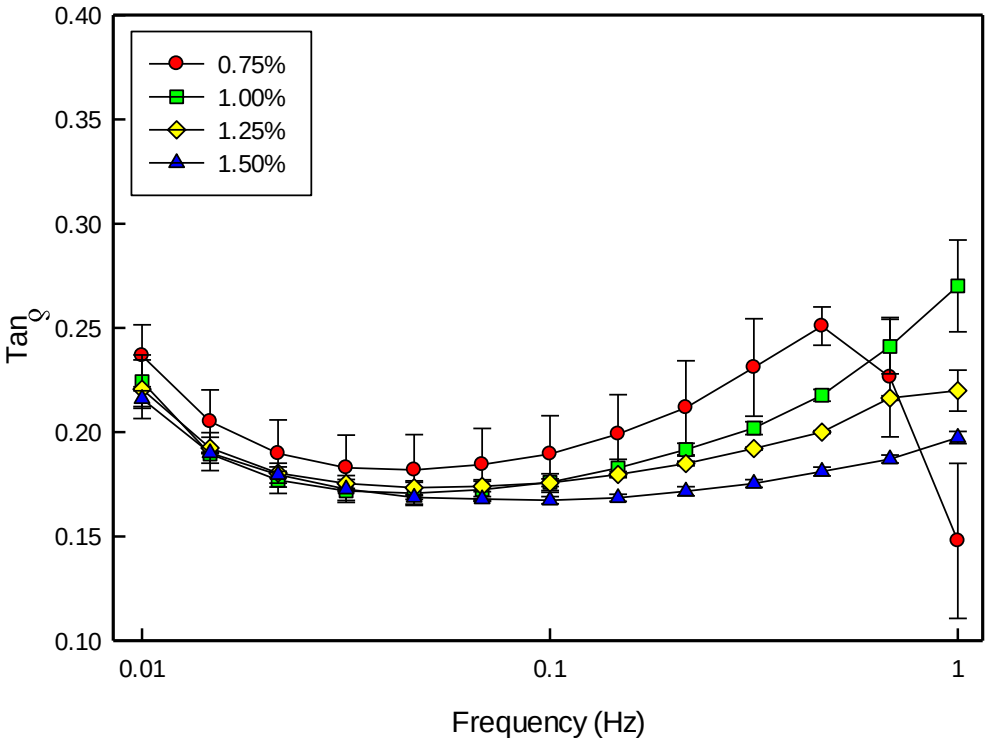

Fig. 3. Frequency dependence of the dynamic moduli for EFH with different pectin concentrations (0.75, 1.00, 1.25, and 1.50%, w/v). (a) Storage modulus, (b) loss modulus, and (c) tan δ.

(a)

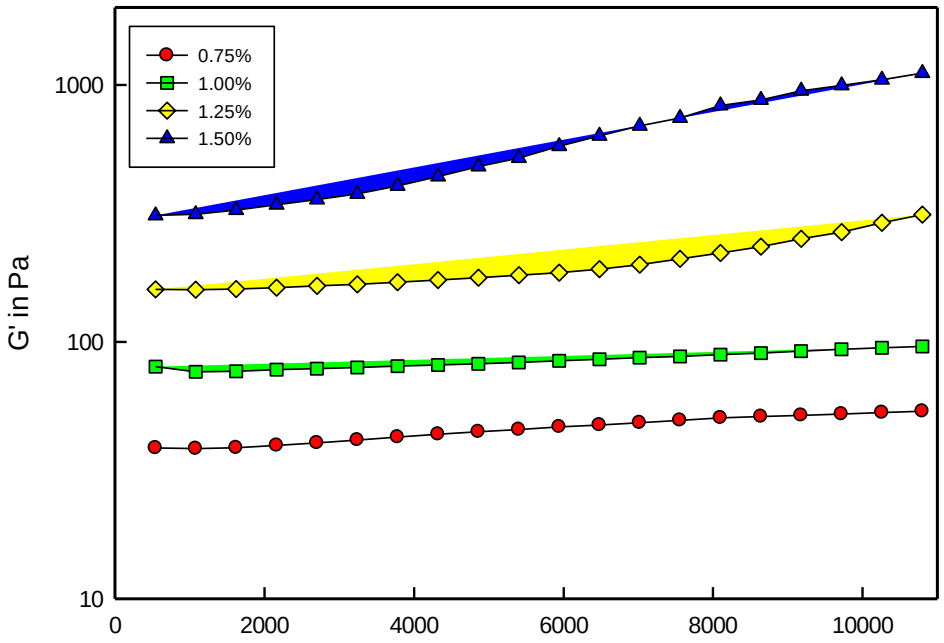
0.75%
1.00%
1.25%
1.50%
G' in Pa
1000
100
10
0
2000
4000
6000
8000
10000

(b)

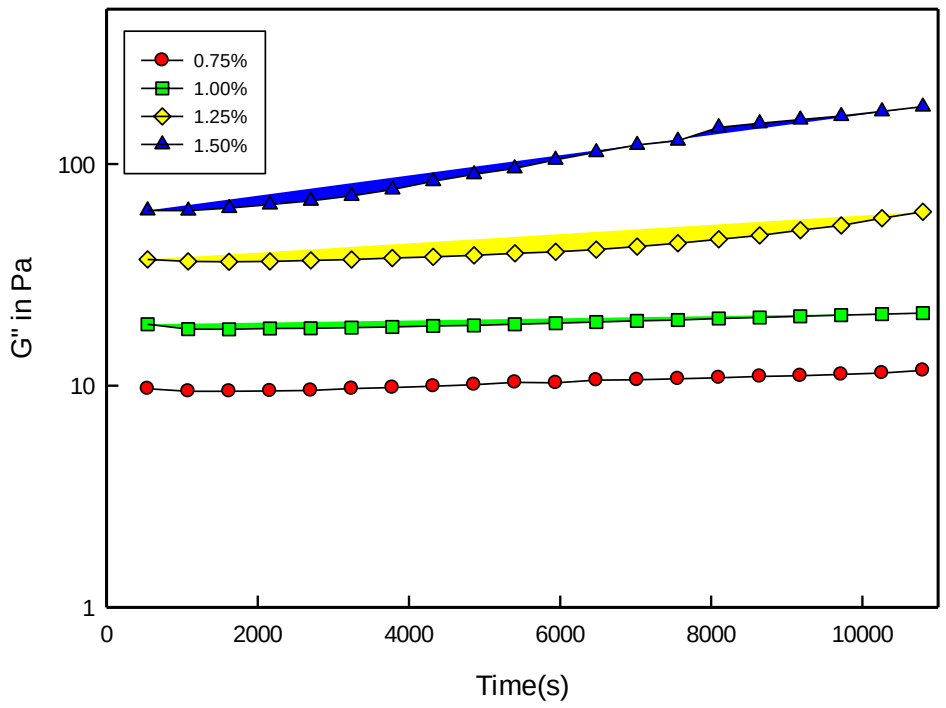
0.75%
1.00%
1.25%
1.50%
G'' in Pa
100
10
1
0
2000
4000
6000
8000
10000
Time(s)

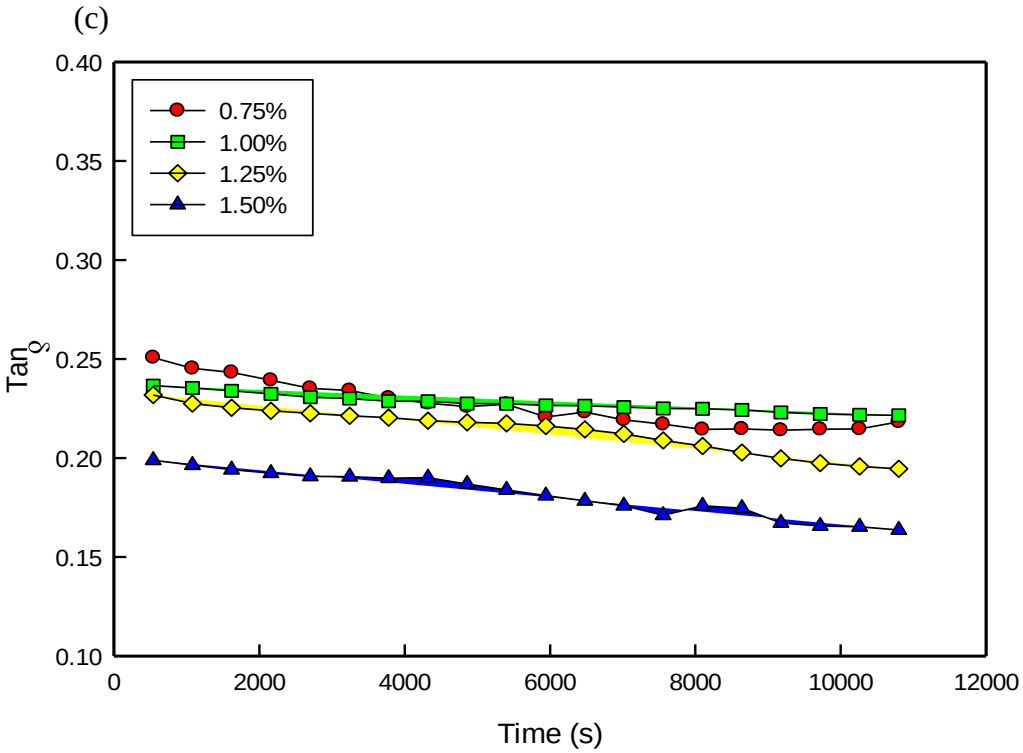

Fig. 4. Time dependence of the dynamic moduli for EFH with different pectin concentrations (0.75, 1.00, 1.25, and 1.50%, w/v). (a) Storage modulus, (b) loss modulus, and (c) tan δ.

Table 1. Effects of pectin concentration on textural parameters of EFH

Pectin concentration (%, w/v)	Hardness (N)	Resilience	Fracturability	Springiness (mm)
0.75	0.47 ± 0.02^{b}	0.04 ± 0.009^{b}	0.07 ± 0.01^{b}	0.57 ± 0.06^{d}
1.00	0.43 ± 0.06^{b}	0.08 ± 0.012^{a}	0.08 ± 0.02^{b}	1.00 ± 0.10^{c}
1.25	0.42 ± 0.04^{b}	0.05 ± 0.009^{ab}	0.07 ± 0.02^{b}	1.45 ± 0.06^{b}
1.50	0.56 ± 0.06^{a}	0.07 ± 0.016^{a}	0.18 ± 0.04^{a}	2.70 ± 0.13^{a}

Data are expressed as the mean ± standard deviation (n = 3). The mean values with different letters in the same column are significantly different ($p < 0.05$).

3.3. Scanning electron microscope (SEM)

SEM was employed to observe the network structure of EFH (Fig. 5). The microstructure of EFH showed different pore sizes depending on the pectin concentrations. It was obvious that pore size decreased as the pectin concentration increased. The pore size in the hydrogel is related to the density of hydrogel matrix. As hydrogel becomes compact, pore size becomes smaller (Moayedzadeh, Khosrowshahi asl, Gunasekaran, & Madadlou, 2018; Voo, Ooi, Islam, Tey, & Chan, 2016). In EFH, it is acknowledged that the chitosan constitutes junction zones and pectin binds along the chitosan (Marianne H. Nordby, 2003; Ventura et al., 2015). Therefore, the increase in pectin concentration seems to have contributed to the formation of compact structure.

(a)

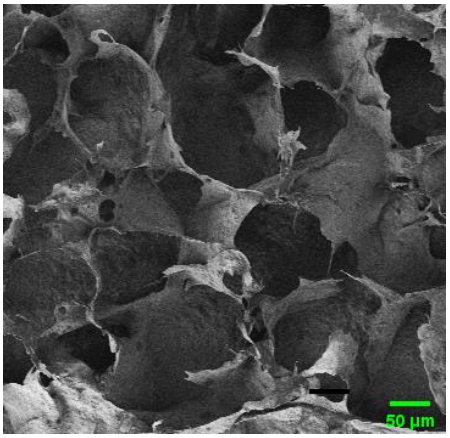

(b)

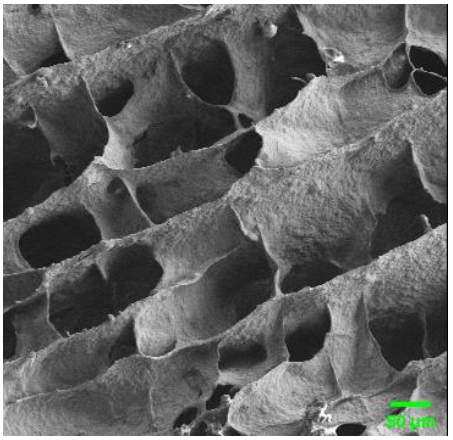

(c)

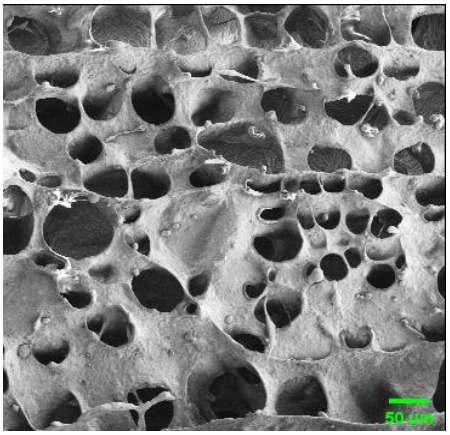

(d)

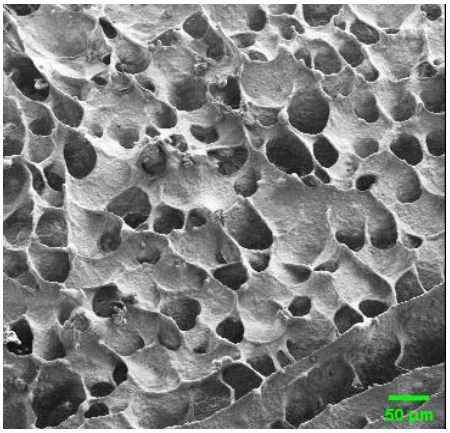

Fig.5. SEM images of EFH with different pectin concentrations. (a) 0.75% pectin, (b) 1.00% pectin, (c) 1.25% pectin, and (d) 1.50% pectin (w/v).

3.4. FT-IR analysis

FT-IR spectroscopy was used to identify the interaction between chitosan and pectin in EFH. The spectra of chitosan and pectin was measured to assign the peaks from chitosan and pectin. In the chitosan spectrum (Fig. 6a), the band at 1,653 cm^{-1} is attributed to amide group of chitosan (*i.e.* amide I) and 1,594 cm^{-1} corresponds to N-H bending of amide II vibration (Rabelo, Tavares, Prata, & Hubinger, 2019). In the spectra of pectin (Fig. 6b), the methyl esterified ($COOCH_3$) group and asymmetric stretching vibration of the carboxylate (COO^-) are assigned to 1,739 cm^{-1} and 1,608 cm^{-1}, respectively (Coimbra et al., 2011; Long, Etxeberria, Nand, Bunt, Ray, & Seyfoddin, 2019; Maciel et al., 2015).

As shown in Fig. 6c, the spectra of EFH in the 1,739 cm^{-1} was not different from that of pectin, indicating that methyl esterified group of pectin did not participate in the interaction. The broadened and shifted band, assigned to vibration region from 3,000 cm^{-1} to 3,600 cm^{-1}, indicated the hydrogen bonds between hydroxyl groups in pectin and hydroxyl/amine groups in chitosan (Kowalonek, 2017; Long et al., 2019). In addition, the broad peak of range from 1,500 cm^{-1} to 1,600 cm^{-1} was attributed to polyelectrolyte between amide group of chitosan and carboxyl group of

pectin (Chen et al., 2010; Lemos, de Souza, & Fajardo, 2021; Rabelo et al., 2019; Rashidova et al., 2004). These results suggest that hydrogel matrix is formed through hydrogen bond and electrostatic interaction between chitosan and pectin. The hydrogen bond between polymers primarily contributed to formation of hydrogel, while electrostatic interaction slightly contributed (Ventura et al., 2015).

In addition, the spectra of EFH showed the peaks at 2,853 cm^{-1} and 2,923 cm^{-1}, which were assigned to the C-H stretching bands of hydrocarbon chains of soybean oil. As compared with the spectra of the hydrogel without emulsion (Fig. 6d), there was no significant difference on the spectra of EFH in the range from 1,500 cm^{-1} to 1,800 cm^{-1}. These results suggest that incorporating the emulsion had no impact on the polymer interactions constituting the hydrogel matrix.

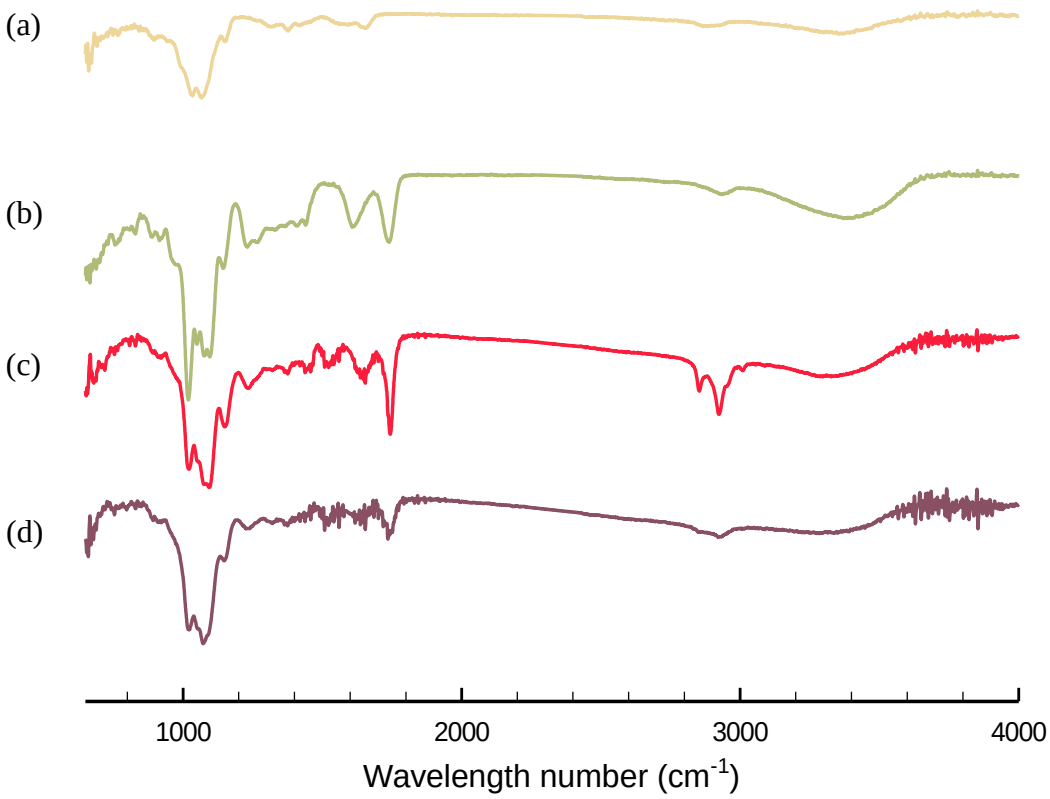

Fig. 6. FT-IR spectra of (a) chitosan, (b) pectin, (c) EFH, and (d) hydrogel without emulsion.

3.5. Release properties of emulsion from hydrogel matrix

The release properties of emulsion were evaluated in the medium pH 2.0 and 7.4. To observe the effect of pH on the release properties, each medium was prepared under the same condition of salts. EFH with 0.75% (w/v) pectin remained intact after exposure to acidic medium for 2 h (Fig. 7a). The similar results were obtained in all the hydrogel with different pectin concentrations (data not shown). On the other hand, disintegration of EFH was observed at pH 7.4, causing increase in the turbidity of medium. EFH with 0.75 and 1.00% (w/v) pectin were completely disrupted, whereas EFH were partially broken and remained in small pieces at 1.25 and 1.50% (w/v) pectin concentrations (data not shown).

As shown in Fig. 7b, the release profiles showed that emulsion was not fully released from the hydrogel matrix when exposed to pH 2.0 medium, regardless of pectin concentrations. In contrast, at pH 7.4 medium, the emulsion was gradually released from the hydrogel matrix, and pectin concentration significantly affected the rate and the extent of emulsion release from the hydrogel matrix. The extent of emulsion release in EFH with 0.75, 1.00, 1.25, and 1.50% pectin was 96.8, 95.6, 87.8, and 65.5%, respectively. The release rate was reduced as the pectin concentration

increased. This could be attributed to the formation of more compact structure as pectin concentration increased, leading to lowering the release rate and the amount of the drug release (Neufeld et al., 2017).

EFH was kept intact in the acidic medium, in which the pH is similar to that in the preparation condition. Thus, it was thought that the change of the functional groups of chitosan and pectin are minimum at the acidic medium, and the interaction between chitosan and pectin was not altered. Accordingly, the network structure of EFH could be maintained, preventing the emulsion release. Meanwhile, at pH 7.4 medium, chitosan is partially neutralized by deprotonation of amine groups ($–NH_2$), whereas carboxyl group (COOH) of pectin is negatively charged since the pK_a of pectin and chitosan is 3.5 and 6.2-7.1, respectively. Thus, at pH 7.4, the electrostatic interaction between chitosan and pectin can be induced, which might maintain the hydrogel network (Martins, de Oliveira, Garcia, Kipper, & Martins, 2018). Nevertheless, EFH was disintegrated during the incubation under the neutral condition.

This phenomenon can be explained by effects of salts on electrostatic interaction between polymers. As shown in Fig. 8, release of emulsion was not observed at pH 7.4 in absence of salt (0 mM of NaCl), showing that

hydrogel matrix was maintained. On the other hand, the emulsion was released in the presence of salt (50-200 mM), indicating that the release of emulsion increased in proportion to the NaCl concentration (50-100 mM). There was no difference in the amount of emulsion release at salt concentrations above 100 mM. It could be attributed that the electrostatic interaction between cationic and anionic polymers are inhibited by salt, resulting in dissociation of hydrogel matrix (Rabelo et al., 2019; C. J. F. Souza, da Costa, Souza, Tosin, & Garcia-Rojas, 2018). These results suggest that the hydrogel matrix control the emulsion release induced by pH and salts, and thus EFH can be used as target delivery system on small intestine.

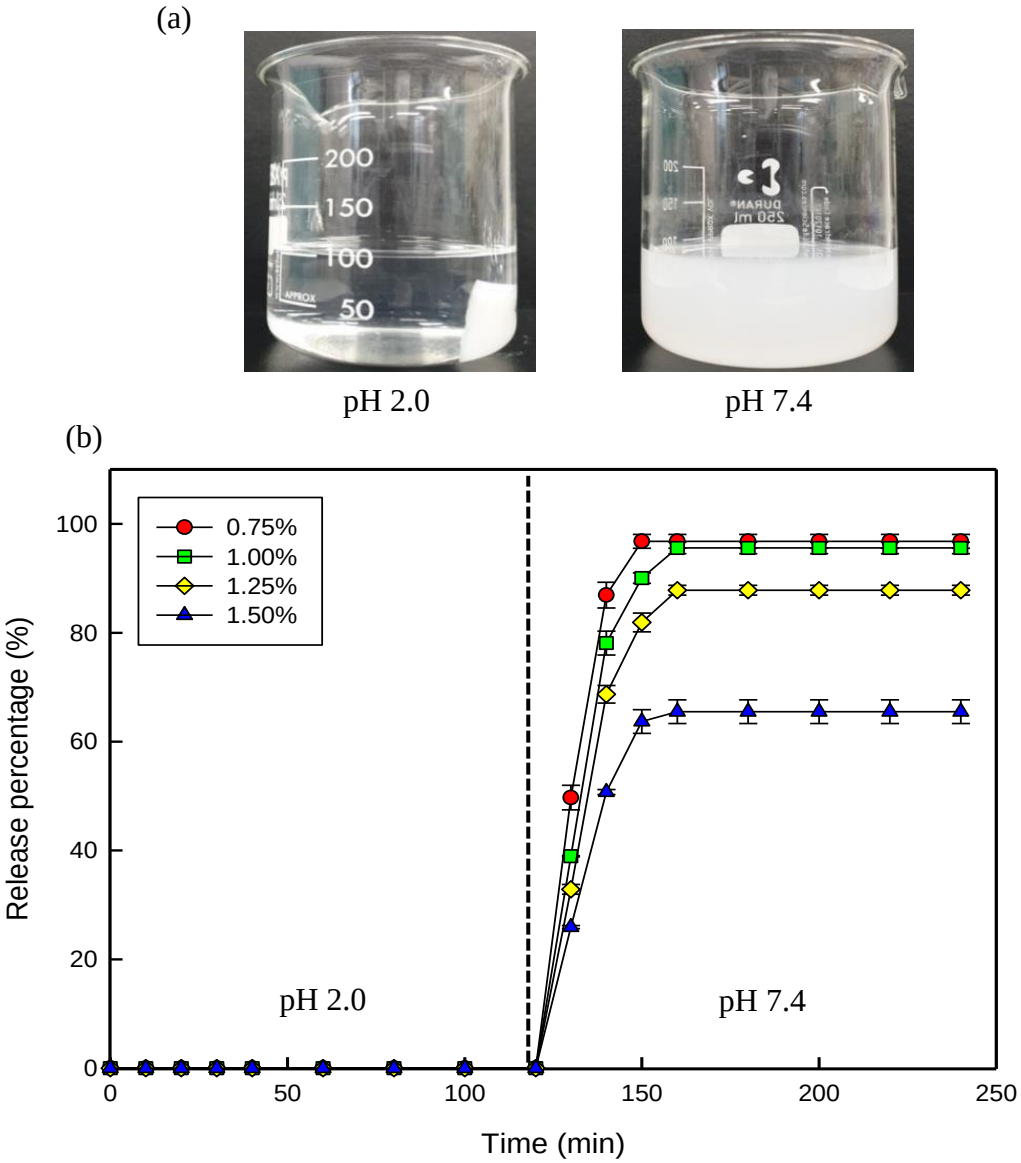

Fig. 7. Release properties of emulsion from hydrogel matrix. (a) Visual appearance of EFH with 0.75% (w/v) pectin after exposed to medium at pH 2.0 and 7.4 for 2 h, and (b) the release profiles of emulsion depending on pectin concentrations (0.75-1.50%, w/v) at pH 2.0 and 7.4.

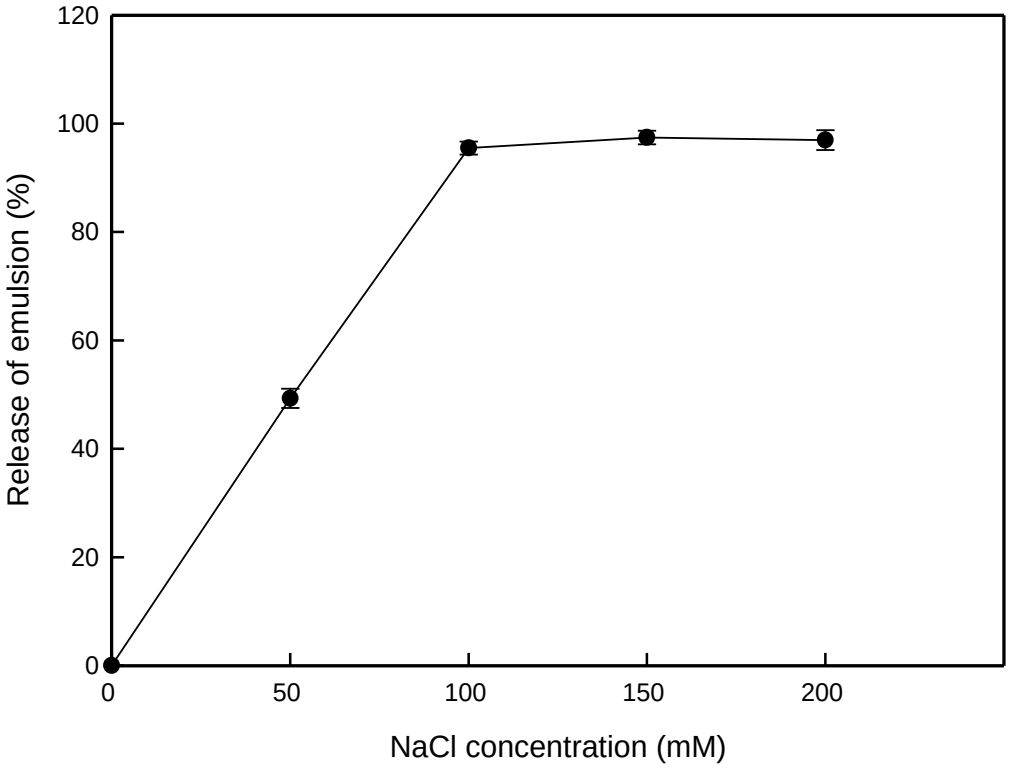

Fig. 8. The effect of salt concentration (0-200 mM) on emulsion release from hydrogel matrix with 0.75% pectin in 100 mM sodium phosphate buffer at pH 7.4 for 2 h.

3.6. FFA release from emulsion and emulsion-filled hydrogel

In the small intestine, lipid droplets are hydrolyzed by lipase, producing FFA and monoacylglycerol. The hydrolysis of triacylglycerol occurs under the adsorption of lipases to the oil/water interfaces (Qian, Decker, Xiao, & McClements, 2012). The release of free fatty acids from emulsion and EFH were shown in Fig. 9. The final extent of FFA release in EFH was 58.67, 55.88, 48.87, and 43.76% at pectin concentrations of 0.75, 1.00, 1.25, and 1.50%, respectively. This result indicated that lipid droplets, which can be hydrolyzed by lipase, decreased as the pectin concentration increased, resulting in reduction of the amount of FFA. It was clearly demonstrated that the high pectin concentration of EFH reduced the release rate and amount of the emulsion (described in section 3.5). Hence, the extent of FFA was lowered as the amount of emulsion, which can be hydrolyzed, decreased. In addition, the high-density hydrogel matrix of EFH may affect the reaction between the lipase and lipid droplets. Diffusion of lipase into EFH could be hindered by polymer networks, and the hydrogel matrix prevented lipase from being placed on the interface of lipid droplets, thus interfering FFA that could be produced. (Corstens et al., 2017; van Leusden, den Hartog, Bast, Postema, van der Linden, & Sagis, 2018).

Compared with emulsion, the significant difference ($p < 0.05$) in the extent of FFA was observed in EFH with 0.75% pectin concentration. It was expected that destabilization of emulsion occurred during the digestion. Destabilization of emulsion is induced by mucin present in gastrointestinal tract, which causes a bridging or depletion flocculation of emulsion (Koukoura et al., 2018; Sarkar et al., 2009; Vingerhoeds, Blijdenstein, Zoet, & van Aken, 2005). In addition, protein hydrolysis occurred on the interfacial protein layer of emulsion by pepsin, resulting in destabilization of emulsion (J. Li et al., 2012; Singh & Sarkar, 2011). Accordingly, due to the destabilization of emulsion, the decrease in the surface area of the lipid droplet retarded the reaction with the lipase, lowering the amount of FFA (Golding et al., 2011; Salvia-Trujillo, Qian, Martin-Belloso, & McClements, 2013; Yi et al., 2014).

It was observed that all EFH were stable during the digestion (*i.e.* no flocculation or coalescence), whereas the emulsion was unstable within the oral digestion and gastric digestion (Fig. 10). This results suggests that the hydrogel matrix prevent emulsion from coalescence and flocculation in the gastric regime, allowing emulsion to reach the small intestine intact (Mun et al., 2015; Torres, Murray, & Sarkar, 2019).

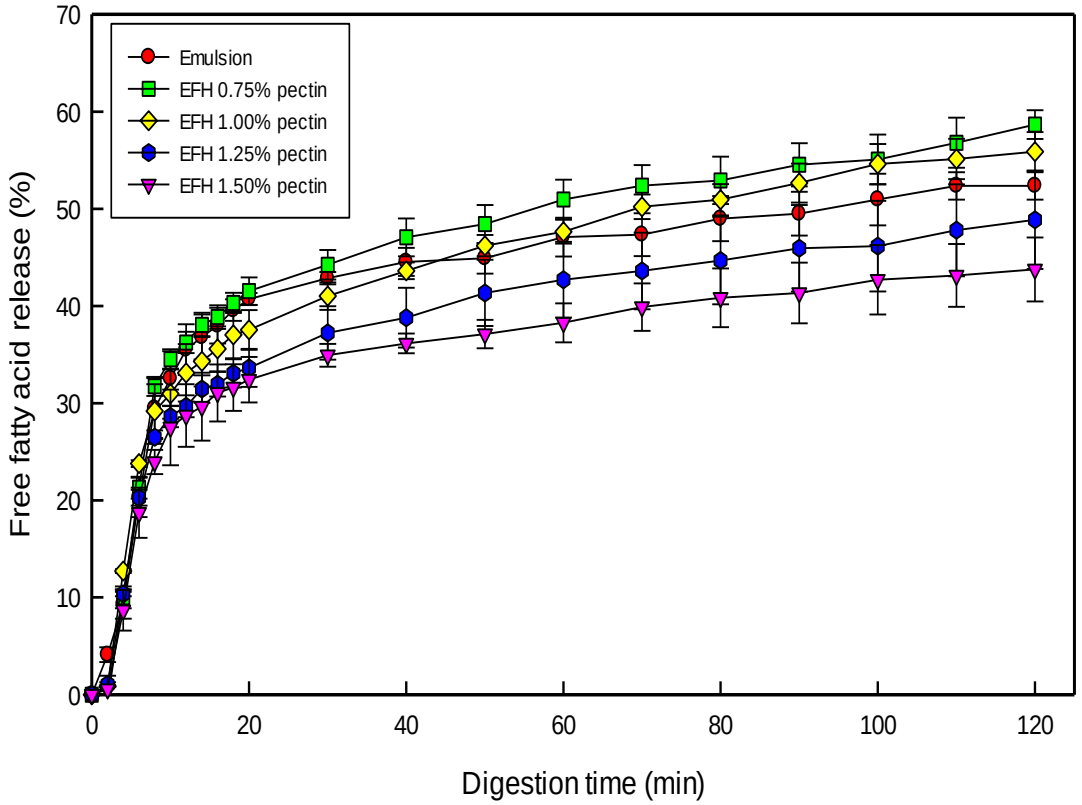

Fig. 9. Release profiles of FFA from EFH with different pectin concentrations (0.75, 1.00, 1.25, and 1.50%, w/v) and sodium caseinate emulsion measured using a pH-stat during small intestinal stage.

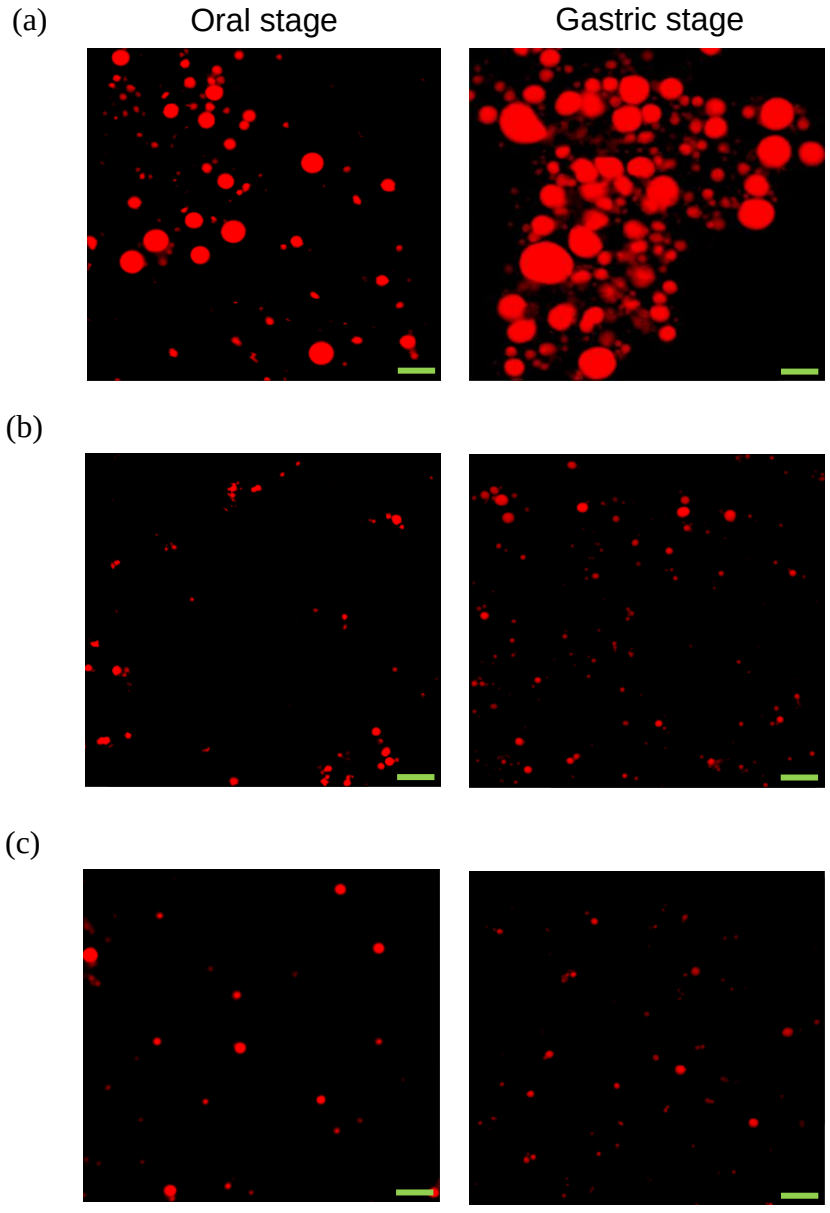
(a)
Oral stage
Gastric stage
(b)
(c)

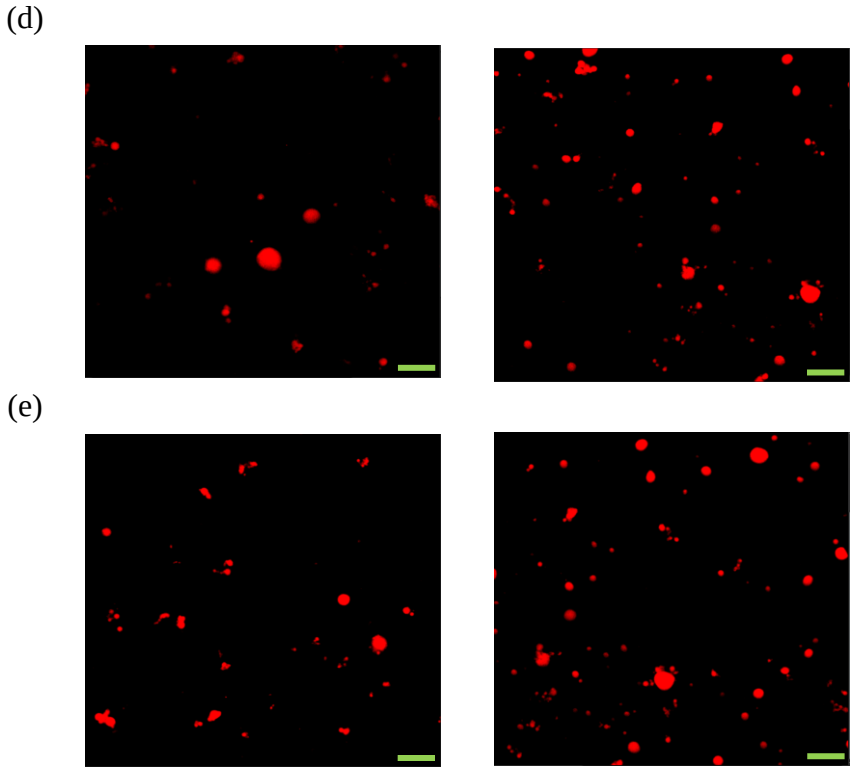

Fig. 10. CLSM images of EFH with different pectin concentrations (0.75-1.50%, w/v) and sodium caseinate emulsion after digestion at oral and gastric stage. (a) Sodium caseinate emulsion, (b) EFH with 0.75% pectin, (c) EFH with 1.00% pectin, (d) EFH with 1.25% pectin, and (e) EFH with 1.50% pectin. The scale bar is 5.0 μm.

3.7. Bioaccessibility of curcumin

The bioaccessilbility is the amount of lipophilic bioactive compounds present in the mixed micelles, which can be absorbed by the epithelial cells (Zheng, Zhang, Peng, & Julian McClements, 2019). In the presence of lipid digestion products, mixed micelles were formed, with bile salts, phospholipids, FFA, and monoglycerides (Porter, Trevaskis, & Charman, 2007; Schwebel, van Hoogevest, Leigh, & Kuentz, 2011; Yao, Xiao, & McClements, 2014). The high digestion of lipid results in formation of large amount of mixed micelle, leading to improve bioaccessibility of the lipophilic bioactive compounds.

As shown in Fig. 11, the bioaccessibility of curcumin incorporated within EFH with different concentrations of pectin was examined after *in vitro* digestion. The bioaccessibility of curcumin in EFH was as follows: 0.75% pectin (23.95 ± 0.8%), 1.00% pectin (21.27 ± 1.6), 1.25% pectin (18.69 ± 0.7), 1.50% pectin (17.38 ± 0.4%). In EFH, the curcumin bioaccessibiliy was decreased as the pectin concentration increased. These results were attributed to result from FFA release test. The decrease of FFA release led to lowering bioaccessibility of curcumin, since there was a few of the curcumin remaining in the lipid and the number of micelles to dissolve curcumin was

decreased. Hence, the amount of curcumin in the micelle fraction of digesta decreased, resulting in reduction of bioaccessibility.

In terms of comparing with emulsion, the bioaccessibility of curcumin was significantly higher in EFH with 0.75% and 1.00% ($p < 0.05$) than that of emulsion (17.25 ± 2.1%). However, there was no significant increase of curcumin bioaccessibility in EFH with pectin concentration (1.25% and 1.50%) compared to emulsion. In EFH, the pectin concentration is significant factor affecting bioaccessibility. Although the stability of emulsion was improved during the digestion in all EFH (0.75-1.50% pectin), the amount of emulsion released in the small intestine decreased as the pectin concentration increased, resulting in reducing the bioaccessibility of curcumin. Therefore, controlling the concentration of pectin is important for developing an effective delivery system.

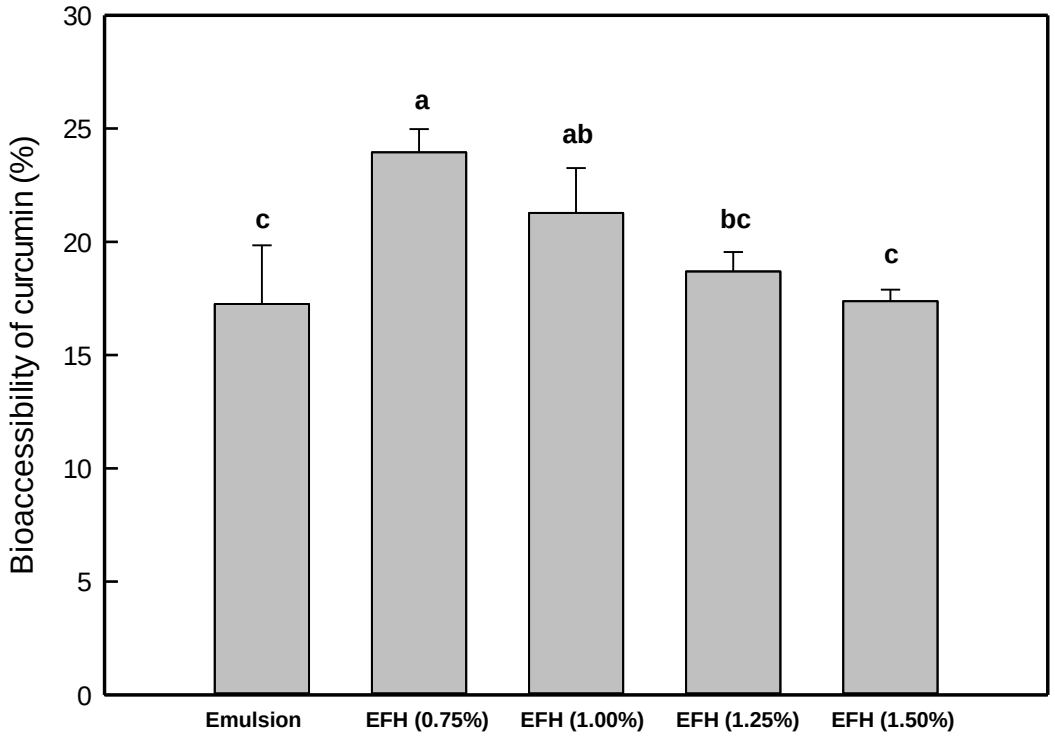

Fig. 11. Bioaccessibility of curcumin in sodium caseinate emulsion and EFH with different pectin concentrations (0.75, 1.00, 1.25, and 1.50%, w/v).

4. Conclusion

In the present study, EFH containing sodium caseinate emulsion was successfully prepared using chitosan and pectin without any chemical agents under the acidic condition. The release of the emulsion occurred at pH 7.4, but did not at pH 2.0. Moreover, the change in the pectin concentration of EFH affected the release property of the emulsion from hydrogel matrix. The increase in pectin concentration resulted in the reduction of the free fatty acid release and bioaccessibility of curcumin in EFH. The curcumin bioaccessibility and lipid digestion in EFH were higher than that in emulsion. It was expected that hydrogel matrix prevent the emulsion from destabilization during the oral and gastric digestion, resulting in increase of bioaccessibility and free fatty acid. EFH could be used as a delivery system of the lipophilic bioactive compounds.

5. Reference

Araiza-Calahorra, A., Akhtar, M., & Sarkar, A. (2018). Recent advances in emulsion-based delivery approaches for curcumin: from encapsulation to bioaccessibility. *Trends in Food Science & Technology, 71*, 155-169.

Chen, P.-H., Kuo, T.-Y., Kuo, J.-Y., Tseng, Y.-P., Wang, D.-M., Lai, J.-Y., & Hsieh, H.-J. (2010). Novel chitosan–pectin composite membranes with enhanced strength, hydrophilicity and controllable disintegration. *Carbohydrate Polymers, 82*(4), 1236-1242.

Coimbra, P., Ferreira, P., de Sousa, H. C., Batista, P., Rodrigues, M. A., Correia, I. J., & Gil, M. H. (2011). Preparation and chemical and biological characterization of a pectin/chitosan polyelectrolyte complex scaffold for possible bone tissue engineering applications. *International Journal of Biological Macromolecules, 48*(1), 112-118.

Corstens, M. N., Berton-Carabin, C. C., Elichiry-Ortiz, P. T., Hol, K., Troost, F. J., Masclee, A. A. M., & Schroën, K. (2017). Emulsion-alginate beads designed to control *in vitro* intestinal lipolysis: towards appetite control. *Journal of Functional Foods, 34*, 319-328.

Farjami, T., & Madadlou, A. (2019). An overview on preparation of

emulsion-filled gels and emulsion particulate gels. *Trends in Food Science & Technology, 86*, 85-94.

Golding, M., Wooster, T. J., Day, L., Xu, M., Lundin, L., Keogh, J., & Clifton, P. (2011). Impact of gastric structuring on the lipolysis of emulsified lipids. *Soft Matter, 7*(7), 3513-3523 .

Hesarinejad, M. A., Koocheki, A., & Razavi, S. M. A. (2014). Dynamic rheological properties of *Lepidium perfoliatum* seed gum: effect of concentration, temperature and heating/cooling rate. *Food Hydrocolloids, 35*, 583-589.

Ilyasoglu, H., & El, S. N. (2014). Nanoencapsulation of EPA/DHA with sodium caseinate–gum arabic complex and its usage in the enrichment of fruit juice. *LWT - Food Science and Technology, 56*(2), 461-468.

Jain, S., Winuprasith, T., & Suphantharika, M. (2020). Encapsulation of lycopene in emulsions and hydrogel beads using dual modified rice starch: characterization, stability analysis and release behaviour during in-vitro digestion. *Food Hydrocolloids, 104*.

Koukoura, E., Panagiotopoulou, M., Pavlou, A., Karageorgiou, V., Fatouros, D. G., Vasiliadou, C., & Ritzoulis, C. (2018). *In vitro* digestion of caseinate and Tween 20 emulsions. *Food Biophysics, 14*(1), 60-68.

Kowalonek, J. (2017). Studies of chitosan/pectin complexes exposed to UV radiation. *International Journal of Biological Macromolecules, 103*, 515-524.

Kumar, M. N. V. R. (2000). A review of chitin and chitosan applications. *Reactive & Functional Polymers, 46*, 1-27.

Lee, K. Y., & Mooney, D. J. (2012). Alginate: properties and biomedical applications. *Progress in Polymer Science, 37*(1), 106-126.

Lei, L., Zhang, Y., He, L., Wu, S., Li, B., & Li, Y. (2017). Fabrication of nanoemulsion-filled alginate hydrogel to control the digestion behavior of hydrophobic nobiletin. *LWT - Food Science and Technology, 82*, 260-267.

Lemos, T. S. A., de Souza, J. F., & Fajardo, A. R. (2021). Magnetic microspheres based on pectin coated by chitosan towards smart drug release. *Carbohydrate Polymers, 265*, 118013.

Li, J., Ye, A., Lee, S. J., & Singh, H. (2012). Influence of gastric digestive reaction on subsequent *in vitro* intestinal digestion of sodium caseinate-stabilized emulsions. *Food & Function, 3*(3), 320-326.

Li, Y., Hu, M., Du, Y., Xiao, H., & McClements, D. J. (2011). Control of lipase digestibility of emulsified lipids by encapsulation within calcium alginate beads. *Food Hydrocolloids, 25*(1), 122-130.

Lim, H.-P., Ho, K.-W., Surjit Singh, C. K., Ooi, C.-W., Tey, B.-T., & Chan, E.-S. (2020). Pickering emulsion hydrogel as a promising food delivery system: synergistic effects of chitosan pickering emulsifier and alginate matrix on hydrogel stability and emulsion delivery. *Food Hydrocolloids, 103*. 105659

Long, J., Etxeberria, A. E., Nand, A. V., Bunt, C. R., Ray, S., & Seyfoddin, A. (2019). A 3D printed chitosan-pectin hydrogel wound dressing for lidocaine hydrochloride delivery. *Materials Science & Engineering C, 104*, 109873.

Lu, Y., Zhang, Y., Yuan, F., Gao, Y., & Mao, L. (2021). Emulsion gels with different proteins at the interface: structures and delivery functionality. *Food Hydrocolloids, 116*. 106637.

Ma, X., & Chatterton, D. E. W. (2021). Strategies to improve the physical stability of sodium caseinate stabilized emulsions: a literature review. *Food Hydrocolloids*. In press.

Maciel, V. B., Yoshida, C. M., & Franco, T. T. (2015). Chitosan/pectin polyelectrolyte complex as a pH indicator. *Carbohydrate Polymers, 132*, 537-545.

Marianne H. Nordby, A.-L. K., Bo Nystrom, Jaan Roots. (2003). Thermoreversible gelation of aqueous mixtures of pectin and chitosan.

Biomacromolecules, 4(2), 337-343.

Martins, J. G., de Oliveira, A. C., Garcia, P. S., Kipper, M. J., & Martins, A. F. (2018). Durable pectin/chitosan membranes with self-assembling, water resistance and enhanced mechanical properties. *Carbohydrate Polymers, 188*, 136-142.

Matalanis, A., & McClements, D. J. (2012). Impact of encapsulation within hydrogel microspheres on lipid digestion: an *In vitro* study. *Food Biophysics, 7*(2), 145-154.

McClements, D. J., Decker, E. A., & Weiss, J. (2007). Emulsion-based delivery systems for lipophilic bioactive components. *Journal of Food Scicence, 72*(8), R109-124.

McClements, D. J., & Li, Y. (2010). Structured emulsion-based delivery systems: controlling the digestion and release of lipophilic food components. *Advanced in Colloid and Interface Science, 159*(2), 213-228.

Moayedzadeh, S., Khosrowshahi asl, A., Gunasekaran, S., & Madadlou, A. (2018). Spontaneous emulsification of fish oil at a substantially low surfactant-to-oil ratio: emulsion characterization and filled hydrogel formation. *Food Hydrocolloids, 82*, 11-18.

Mun, S., Kim, Y.-R., Shin, M., & McClements, D. J. (2015). Control of lipid

digestion and nutraceutical bioaccessibility using starch-based filled hydrogels: Influence of starch and surfactant type. *Food Hydrocolloids, 44*, 380-389.

Neufeld, L., & Bianco-Peled, H. (2017). Pectin-chitosan physical hydrogels as potential drug delivery vehicles. *International Journal of Biological Macromolecules, 101*, 852-861.

Pan, Y., Xie, Q. T., Zhu, J., Li, X. M., Meng, R., Zhang, B., Jin, Z. Y. (2019). Study on the fabrication and *in vitro* digestion behavior of curcumin-loaded emulsions stabilized by succinylated whey protein hydrolysates. *Food Chemistry, 287*, 76-84.

Parhi, R. (2017). Cross-linked hydrogel for pharmaceutical applications: a review. *Advanced Pharmaceutical Bulletin, 7*(4), 515-530.

Perugini, L., Cinelli, G., Cofelice, M., Ceglie, A., Lopez, F., & Cuomo, F. (2018). Effect of the coexistence of sodium caseinate and Tween 20 as stabilizers of food emulsions at acidic pH. *Colloids and Surfaces B: Biointerfaces, 168*, 163-168.

Porter, C. J., Trevaskis, N. L., & Charman, W. N. (2007). Lipids and lipid-based formulations: optimizing the oral delivery of lipophilic drugs. *Nature Reviews Drug Discovery, 6*(3), 231-248.

Qian, C., Decker, E. A., Xiao, H., & McClements, D. J. (2012).

Nanoemulsion delivery systems: influence of carrier oil on beta-carotene bioaccessibility. *Food Chemistry, 135*(3), 1440-1447.

Rabelo, R. S., Tavares, G. M., Prata, A. S., & Hubinger, M. D. (2019). Complexation of chitosan with gum arabic, sodium alginate and kappa-carrageenan: effects of pH, polymer ratio and salt concentration. *Carbohydrate Polymers, 223*, 115120.

Raikos, V., & Ranawana, V. (2017). Designing emulsion droplets of foods and beverages to enhance delivery of lipophilic bioactive components - a review of recent advances. *International Journal of Food Science & Technology, 52*(1), 68-80.

Rashidova, S. S., Milusheva, R. Y., Semenova, L. N., Mukhamedjanova, M. Y., Voropaeva, N. L., Vasilyeva, S., Ruban, I. N. (2004). Characteristics of interactions in the pectin-chitosan system. *Chromatographia, 59*(11-12).

Salminen, H., Bischoff, S., & Weiss, J. (2019). Impact of concentration ratio on the formation and stability of emulsions stabilized by quillaja saponin – sodium caseinate mixtures. *Food Biophysics, 14*(2), 109-119.

Salvia-Trujillo, L., Qian, C., Martin-Belloso, O., & McClements, D. J. (2013). Influence of particle size on lipid digestion and beta-carotene

bioaccessibility in emulsions and nanoemulsions. *Food Chemistry, 141*(2), 1472-1480.

Sarkar, A., Goh, K. K. T., & Singh, H. (2009). Colloidal stability and interactions of milk-protein-stabilized emulsions in an artificial saliva. *Food Hydrocolloids, 23*(5), 1270-1278.

Sarker, B., Papageorgiou, D. G., Silva, R., Zehnder, T., Gul, E. N. F., Bertmer, M., . . . Boccaccini, A. R. (2014). Fabrication of alginate-gelatin crosslinked hydrogel microcapsules and evaluation of the microstructure and physico-chemical properties. *Journal of Materials Chemistry B, 2*(11), 1470-1482.

Schwebel, H. J., van Hoogevest, P., Leigh, M. L., & Kuentz, M. (2011). The apparent solubilizing capacity of simulated intestinal fluids for poorly water-soluble drugs. *Pharmaceutical Development and Technology, 16*(3), 278-286.

Silva, K. C. G., Bourbon, A. I., Pastrana, L., & Sato, A. C. K. (2020). Emulsion-filled hydrogels for food applications: influence of pH on emulsion stability and a coating on microgel protection. *Food & Function, 11*(9), 8331-8341.

Singh, H., & Sarkar, A. (2011). Behaviour of protein-stabilised emulsions under various physiological conditions. *Advanced in Colloid and*

Interface Science, 165(1), 47-57.

Souza, C. J. F., da Costa, A. R., Souza, C. F., Tosin, F. F. S., & Garcia-Rojas, E. E. (2018). Complex coacervation between lysozyme and pectin: effect of pH, salt, and biopolymer ratio. *International Journal of Biological Macromolecules, 107*(Pt A), 1253-1260.

Souza, C. J. F., & Garcia-Rojas, E. E. (2015). Effects of salt and protein concentrations on the association and dissociation of ovalbumin-pectin complexes. *Food Hydrocolloids, 47*, 124-129.

Surjit Singh, C. K., Lim, H. P., Tey, B. T., & Chan, E. S. (2021). Spray-dried alginate-coated pickering emulsion stabilized by chitosan for improved oxidative stability and *in vitro* release profile. *Carbohydrate Polymers, 251*, 117110.

Tang, Y.-F., Du, Y.-M., Hu, X.-W., Shi, X.-W., & Kennedy, J. F. (2007). Rheological characterisation of a novel thermosensitive chitosan/poly(vinyl alcohol) blend hydrogel. *Carbohydrate Polymers, 67*(4), 491-499.

Torres, O., Murray, B. S., & Sarkar, A. (2019). Overcoming *in vitro* gastric destabilisation of emulsion droplets using emulsion microgel particles for targeted intestinal release of fatty acids. *Food Hydrocolloids, 89*, 523-533.

Ulubayram, K., Aksu, E., Gurhan, S. I., Serbetci, K., & Hasirci, N. (2002). Cytotoxicity evaluation of gelatin sponges prepared with different cross-linking agents. *Journal of Biomaterials Science, Polymer Edition, 13*(11), 1203-1219.

van Leusden, P., den Hartog, G. J. M., Bast, A., Postema, M., van der Linden, E., & Sagis, L. M. C. (2018). Lipase diffusion in oil-filled, alginate micro- and macrobeads. *Food Hydrocolloids, 85*, 242-247.

Ventura, I., & Bianco-Peled, H. (2015). Small-angle X-ray scattering study on pectin-chitosan mixed solutions and thermoreversible gels. *Carbohydrate Polymers, 123*, 122-129.

Vingerhoeds, M. H., Blijdenstein, T. B. J., Zoet, F. D., & van Aken, G. A. (2005). Emulsion flocculation induced by saliva and mucin. *Food Hydrocolloids, 19*(5), 915-922.

Voo, W.-P., Ooi, C.-W., Islam, A., Tey, B.-T., & Chan, E.-S. (2016). Calcium alginate hydrogel beads with high stiffness and extended dissolution behaviour. *European Polymer Journal, 75*, 343-353.

Yao, M., Xiao, H., & McClements, D. J. (2014). Delivery of lipophilic bioactives: assembly, disassembly, and reassembly of lipid nanoparticles. *Annual Review of Food Science Technology, 5*, 53-81.

Yi, J., Li, Y., Zhong, F., & Yokoyama, W. (2014). The physicochemical

stability and *in vitro* bioaccessibility of beta-carotene in oil-in-water sodium caseinate emulsions. *Food Hydrocolloids, 35*, 19-27.

Zheng, B., Zhang, X., Peng, S., & Julian McClements, D. (2019). Impact of curcumin delivery system format on bioaccessibility: nanocrystals, nanoemulsion droplets, and natural oil bodies. *Food & Function*, *10*(7), 4339-4349.

국문 초록

수중유적형 에멀젼은 친유성 생리활성 물질의 운반체로서 널리 사용되어오고 있다. 그러나 에멀젼은 소화과정 중 불안정화가 발생하고 이는 생리활성 물질의 생체이용률에 영향을 미치게 된다. 최근 운반 시스템을 활용하여 위장관 내 에서 에멀젼의 안정성을 향상시키고 생리활성물질의 생체이용률을 높이기 위한 연구가 이루어지고 있다. 본 연구에서는 산성조건에서 화학적 물질을 사용하지 않고 cold-set 겔화를 이용한 에멀젼-함입 하이드로겔을 제조하였다. 키토산과 펙틴을 하이드로겔 구조체로서 사용하고 카제인 나트륨을 유화제로서 사용하였다. 점탄성 측정을 통해 펙틴 농도가 0.75-1.50% (w/v) 범위에서 증가함에 따라 저장탄성률이 증가하였다. 미세구조 관찰결과, 펙틴 농도 증가에 따라 하이드로겔 내부 기공의 크기가 감소하고 더 조밀한 하이드로겔 구조가 생성되는 것을 확인하였다. FT-IR 분석을 이용하여 에멀젼-함입 하이드로겔을 구성하는 키토산과 펙틴간의 결합을 규명하였다. 키토산과 펙틴간의 수소결합과 정전기적결합은 각각 3,326 cm^{-1} 과 1,500-1,600 cm^{-1} 에 존재함을 확인하였다. 또한 하이드로겔 내부에 에멀젼의

존재 유무는 하이드로겔을 구성하는 고분자간의 결합에 영향을 주지 않았다. 하이드로겔 구조체로부터 에멀젼은 pH 2.0 에서 방출되지 않은 반면 pH 7.4 에서는 하이드로겔이 붕괴되면서 에멀젼이 방출되는 것을 관찰하였다. 또한 에멀젼-함입 하이드로겔의 방출특성은 펙틴농도에 영향을 받는 것을 확인하였다. 소화모델 내에서 에멀젼 및 에멀젼-함입 하이드로겔로부터 생성되는 자유지방산을 평가하였다. 에멀젼-함입 하이드로겔에서 방출된 자유지방산은 0.75, 1.00, 1.25 그리고 1.50% 펙틴농도에서 각각 58.67, 55.88, 48.87 및 43.76% 였다. 에멀젼과 비교하였을 때, 0.75% 펙틴을 함유하는 에멀젼-함입 하이드로겔에서의 방출된 자유지방산의 양이 에멀젼보다 더 높았다. 공초점 레이저 주사현미경을 이용하여 소화모델 내 구강 단계 및 위장 단계에서 에멀젼이 하이드로겔 구조체에 의해 불안정해 지지 않은 것을 관찰 하였다. 커큐민을 지용성 생리활성물질의 지표물질로서 사용하여 소장소화 후 bioaccessibility 를 평가하였다. 에멀젼-함입 하이드로겔에 포집된 커큐민의 bioaccessibility 는 펙틴 농도가 증가함에 따라 감소하였고 0.75% 펙틴 농도를 함유한 에멀젼-함입 하이드로겔에서 에멀젼에 함입되

었을 때 보다 1.38 배 증가하는 결과가 나타났다. 본 연구에서 에멀젼 함입 하이드로겔은 위장관 내에서 에멀젼의 안정성을 개선함으로써 생리활성물질의 bioaccessibility 를 향상시킨 것을 입증했다. 결론적으로 에멀젼-함입 하이드로겔은 식품산업에서 친유성 생리활성물질들 위한 운반 시스템으로서 활용될 것으로 사료된다.

주제어: 키토산, 펙틴, 에멀젼-함입 하이드로겔, 운반 시스템, 카제인 나트륨 에멀젼, bioaccessibility

학번: 2019-21740